Cosmological baryon diffusion and nucleosynthesis

James H. Applegate
Department of Astronomy, Columbia University, New York, New York 10027

Craig J. Hogan
Steward Observatory, University of Arizona, Tucson, Arizona 85721

Robert J. Scherrer
Department of Physics, University of Chicago, 5641 South Ellis Avenue, Chicago, Illinois 60637
(Received 9 October 1986)

The diffusion rate of baryons through the big-bang plasma is calculated. Fluctuations in baryon density in the early Universe lead to inhomogeneities in the neutron-proton ratio, due to the differential diffusion of these particles through the radiation plasma. For certain types of nonlinear fluctuations, some nucleosynthesis would occur in very neutron-rich regions. Nuclear products of homogeneous neutron-enriched regions are evaluated numerically using a standard reaction network and these results are used to estimate final abundances in an inhomogeneous universe. Net deuterium and lithium abundances tend to increase and the net helium abundance tends to decrease compared to an unperturbed standard model. It is suggested that pronounced nonlinear baryon-density fluctuations produced in QCD- or electroweak-epoch phase transitions could alter abundances sufficiently to make a closed baryonic universe consistent with current observations of these elements. In such a model the abundance of heavier elements (C,N,O, etc.) increases significantly and approaches observable levels. Abundances can be used to place constraints on extreme scenarios for phase transitions at these epochs.

I. INTRODUCTION

It has become a standard argument of big-bang cosmology that the Universe cannot possibly be closed with baryons because of the unacceptable consequences for nucleosynthesis. The most direct confrontations with observations come from the excessive helium and inadequate deuterium production.[1,2] The conflict of a closed baryonic universe model with the deuterium observations is several orders of magnitude, and the conflict with helium observations, although only a few percent, also appears well established. There are many ways to alter abundances during or after the big bang, but such schemes are generally unsatisfying or implausible as they add extra complicated ingredients, such as sources of γ rays to photodissociate helium[3–6] or special environments where neutrons can be cooked off of nuclei and quickly transported to cool environments where they can form deuterium before decaying.[7] Moreover, these models seldom solve the deuterium and helium problems simultaneously. There has been a feeling that the standard big bang with low baryon density provides the most natural environment for making the light-element abundances come out right.

Are there "natural" ways to alter the standard model to increase deuterium and decrease helium production in the big bang itself? One alternative is to presuppose that there were inhomogeneities in the baryon distribution at the time of nucleosynthesis. Epstein and Petrosian[8] showed that large-scale nonlinear inhomogeneities do indeed alter the abundances, but in the wrong direction to reconcile a closed baryonic universe with observations. However, Applegate and Hogan[9] showed that nonlinear structures produced by cavitation during the QCD phase transition would occur on a smaller scale where they would lead to the segregation of neutrons and protons at nucleosynthesis, and argued that in this situation one might indeed expect deuterium and helium production to change in the sense of mimicking a low-baryon-density universe. In this paper we investigate this idea more carefully and confirm their expectation. The theory of baryon diffusion in Sec. II provides the quantitative basis for a description of segregation effects (Sec. III) which characterizes the scale, morphology, and amplitude of baryon-density perturbation necessary for significant local neutron enrichment at nucleosynthesis. In Sec. IV we present the results of numerical computations of abundances produced in neutron-rich regions, and discuss these results in terms of constraints on the mean baryon density and on the nature of the baryon-density perturbations. Section V examines the possibility of further refinement in our conclusions.

It is possible, given the current uncertainty remaining over the nature of the QCD transition and others, that these segregation effects might not be pronounced enough to perturb standard nucleosynthesis significantly. It cannot however be argued that they constitute an artificial new ingredient in the standard cosmological model, since they arise automatically at some level if the QCD phase transition is first order and its supercooling and nucleation happen in the most naive way[10–12] (e.g., without being strongly affected by unknown impurities). In fact any first-order transition occurring at less than several hundred GeV (for example, the electroweak phase transition) can also, in principle, cause neutron-proton segregation. The basic requirement is that nonlinear perturbations in baryon density appear on a comoving scale larger than the proton diffusion length but smaller than the neutron diffusion length at nucleosynthesis.

The primary goal of the present work is to define more precisely the abundance perturbations that are produced by idealized baryon-density perturbation so as to understand better the range of possible effects on the standard cosmological model. We do not study in detail the processes occurring during the phase transitions which produce the perturbations, but assume perturbations of various scales and configurations and study their effects on nucleosynthesis. We emphasize one particular type of new nucleosynthesis effect which emerges as particularly interesting: nucleosynthesis in neutron-enriched regions.[13] Neutron-rich nucleosynthesis produces the most interesting departures from the standard model: namely, vastly increased production of deuterium and a reduction in the net helium yield. A surprising bonus is that it also produces observable abundances of heavier elements such as carbon, suggesting that these elements can also be used in some circumstances as cosmological constraints.

II. THE DIFFUSION OF NEUTRONS AND PROTONS

Upper and lower limits to scales on which a perturbation in baryon density can affect nucleosynthesis through neutron-proton segregation are determined by the comoving diffusion lengths of neutrons and protons at the onset of nucleosynthesis. At high temperatures the diffusion lengths of neutrons and protons are equal because these particles intertransmute rapidly through weak interactions. After the weak interactions have fallen out of equilibrium, nucleons retain their identity as neutrons or protons and diffusive segregation can occur. Coulomb collisions between protons and electrons (or positrons) give a proton transport cross section roughly equal to the Thomson cross section. Neutrons scatter electrons with a cross section $\sim 10^{-30}\,\mathrm{cm}^2$ because of their magnetic moment, and they scatter protons with a cross section $\sim 10^{-23}\,\mathrm{cm}^2$. These numbers show that the mean free path of the neutron is roughly 10^6 times that of the proton. In the remainder of this section we compute the diffusion coefficients and diffusion lengths for neutrons and protons, and determine the scales on which diffusive separation can occur.

Consider the diffusion of neutrons. If the decay of the neutron and the expansion of the Universe are neglected, the neutron density n is described by

$$\frac{\partial n}{\partial t} = D_n \nabla^2 n \ , \tag{1}$$

where D_n is the (constant) diffusion coefficient. After a time t the rms distance d a neutron has diffused is given by[14]

$$d = (6 D_n t)^{1/2} \ . \tag{2}$$

Since the diffusion coefficient depends on temperature and baryon density it becomes a known function of time $D(t)$ in an expanding universe. To allow for this we write

$$D(t) = D_0 f(t) \ , \tag{3}$$

where D_0 is a constant and $f(t)$ is a dimensionless function of time. We define a new time coordinate $u(t)$ by

$$du = f(t) dt \ . \tag{4}$$

With this, the diffusion equation is transformed into

$$\frac{\partial n}{\partial u} = D_0 \nabla^2 n \ . \tag{5}$$

Thus after a time t in an expanding universe the rms distance diffused by a neutron is

$$d = [6 D_0 u(t)]^{1/2} \ . \tag{6}$$

We normalize the scale factor $a(t)$ to $a = 1$ when the neutrino temperature T_ν is 1 MeV. Since T_ν evolves as $aT_\nu = \mathrm{const}$ through e^+e^- annihilation, the comoving diffusion length is given by

$$\frac{d}{a} = T_\nu(\mathrm{MeV}) [6 D_0 u(t)]^{1/2} \ . \tag{7}$$

The diffusion of nucleons while the weak interactions are in equilibrium can be described simply by noting that all the diffusion occurs while the nucleon is a neutron. In equilibrium, a nucleon spends a fraction $X_n(T)$ of its time as a neutron, where

$$X_n = (1 + e^{Q/T})^{-1} \tag{8}$$

and $Q = 1.29$ MeV is the neutron-proton mass difference. The diffusion of nucleons is described by

$$\frac{\partial n}{\partial t'} = D_n \nabla^2 n \ , \tag{9}$$

where n is the density of nucleons, D_n is the neutron diffusion coefficient, and t' is a time coordinate related to the time t by

$$dt' = X_n dt \ . \tag{10}$$

Neutrons and protons go their separate ways once the weak interactions decouple. We assume that the weak interactions are in equilibrium down to a temperature $T_{\mathrm{weak}} = 794$ keV, and decouple instantaneously once the electron temperature falls below this value. We choose this temperature because the equilibrium neutron abundance, Eq. (8), and the asymptotic neutron abundance found by Peebles[15] when he neglects neutron decay are equal at $T = 794$ keV. The slopes of the comoving diffusion lengths shown in Fig. 1 are discontinuous at T_{weak} because of our assumption of instantaneous weak decoupling. The rapid increase of the neutron diffusion length for $T < T_{\mathrm{weak}}$ is due to the fact that neutrons spend all of their time as neutrons for $T < T_{\mathrm{weak}}$, whereas for $T > T_{\mathrm{weak}}$ they spend a fraction X_n of their time as a neutron.

Neutrons are scattered by electrons and positrons and by protons. Other scattering mechanisms, such as neutron-photon scattering, neutron-neutron scattering, and the absorption and reemission of neutrons by the formation and subsequent photodissociation of deuterium, may be neglected. If D_{ne} is the neutron diffusion coeffi-

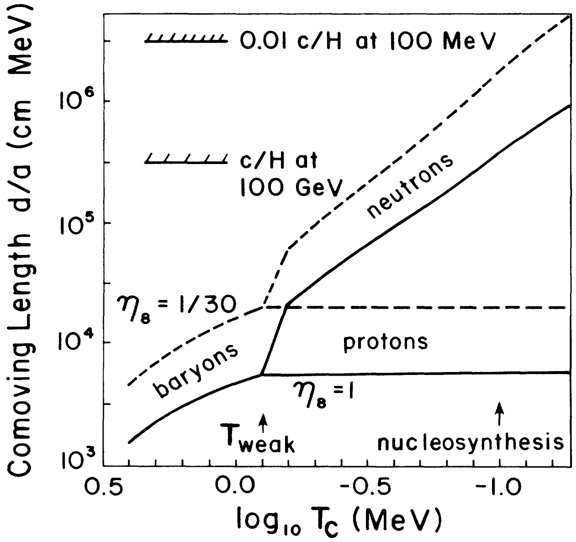

FIG. 1. Comoving diffusion distance as a function of Hubble time or temperature. The solid curve shows the rms comoving distance $d(T)/a$ (normalized to $a=1$ at $T=1$ MeV) traveled by a baryon up to time T. After weak decoupling, neutron and proton transport are shown separately. Also shown are the characteristic scale expected for QCD cavitation and the electroweak horizon scale.

cient appropriate for electron scattering only, and D_{np} is the diffusion coefficient for neutron-proton scattering, then the neutron diffusion coefficient D_n is given by

$$D_n{}^{-1}=D_{ne}{}^{-1}+D_{np}{}^{-1} . \tag{11}$$

Consider neutron-electron scattering. The structure of the neutron necessitates the replacement of the bare electromagnetic vertex $ie\gamma_\mu$ with $ie\Gamma_\mu(q^2)$, where[16]

$$\Gamma_\mu(q^2)=\gamma_\mu F_1(q^2)+\frac{i\kappa}{2M}F_2(q^2)\sigma_{\mu\nu}q^\nu . \tag{12}$$

Here M is the neutron mass, q^ν is the four-momentum transferred, F_1 and F_2 are the Dirac and Pauli form factors, $\sigma_{\mu\nu}=\frac{1}{2}i[\gamma_\mu,\gamma_\nu]$, and $\kappa=-1.91$ is the anomalous magnetic moment of the neutron in nuclear magnetons. At the low energies we consider the form factors can be evaluated at $q^2=0$; thus $F_1=0$ and $F_2=1$. Our vertex is

$$\Gamma_\mu=\frac{i\kappa}{2M}\sigma_{\mu\nu}q^\nu . \tag{13}$$

We assume that the electron energy is much less than M, but we allow the electron energy and mass to be comparable. With this assumption, the differential cross section is

$$\frac{d\sigma}{d\Omega}=\frac{\alpha^2\kappa^2}{4M^2}[1+\csc^2(\theta/2)] , \tag{14}$$

where θ is the scattering angle. The transport cross section σ_t, defined by

$$\sigma_t=\int d\Omega\frac{d\sigma}{d\Omega}(1-\cos\theta) , \tag{15}$$

is

$$\sigma_t=3\pi\left[\frac{\alpha\kappa}{M}\right]^2=8\times10^{-31}\,\text{cm}^2 . \tag{16}$$

The diffusion coefficient for heavy particles diffusing through a gas of light particles may be found by computing the mobility of the heavy particles.[17] The mobility b is given by

$$\mathbf{V}=b\mathbf{F} , \tag{17}$$

where $\mathbf{F}$ is the force applied to a heavy particle and $\mathbf{V}$ is the terminal velocity of the particle in the medium. The diffusion coefficient is related to the mobility by Einstein's relation[14]

$$D=bT . \tag{18}$$

The drag force $\mathbf{F}_r$ on a neutron moving with velocity $\mathbf{V}$ through the electron-positron plasma is

$$\mathbf{F}_r=4\int\frac{d^3p}{(2\pi\hbar)^3}f(\mathbf{v}+\mathbf{V})v\mathbf{p}\sigma_t , \tag{19}$$

where $f(\mathbf{V}+\mathbf{v})$ is the electron-positron distribution in the rest frame of the neutron. We assume that the velocity of the neutron is much less than that of an electron or positron, and we assume that the distribution function $f(\mathbf{v}+\mathbf{V})$ reduces to a Maxwellian distribution when $\mathbf{V}=0$. We obtain

$$b^{-1}=\frac{2}{T}\int\frac{p^2dp}{3\pi^2\hbar^3}vp^2\sigma_t e^{-E/T} . \tag{20}$$

The diffusion coefficient is obtained by combining Eqs. (16), (18), and (20):

$$D_{ne}=\frac{\pi}{16}\left[\frac{M}{m_e}\right]^2\left[\frac{\hbar}{m_e}\right]\frac{1}{(\alpha\kappa)^2}\frac{e^{1/x}}{xf(x)} \tag{21}$$

or

$$D_{ne}=2.01\times10^{10}\frac{e^{1/x}}{xf(x)}\frac{\text{cm}^2}{\text{sec}} ,$$

where $x=T/m_ec^2$ and $f(x)=1+3x+3x^2$.

We introduce negligible error by assuming the pairs have a Maxwellian distribution instead of a Fermi-Dirac one with $\mu=0$ (note that μ includes the rest mass). It is most important to know D_n near the onset of nucleosynthesis; at this time $T=0.2m_ec^2$, so the distribution function is almost at Maxwellian distribution. Even at high temperatures $T\gg m_ec^2$, the error is only 3%.

At energies below a few MeV the neutron-proton interaction is dominated by s-wave scattering, and the cross section may be parametrized using effective range theory. The n-p cross section is[18]

$$\sigma_{np}=\frac{\pi a_s{}^2}{(a_sk)^2+(1-\frac{1}{2}r_sa_sk^2)^2}+\frac{3\pi a_t{}^2}{(a_tk)^2+(1-\frac{1}{2}r_ta_tk^2)^2} . \tag{22}$$

The singlet and triplet state scattering lengths a_s,a_t and effective ranges r_s,r_t are[18]

$$a_s = -23.71 \text{ fm}, \quad a_t = 5.432 \text{ fm} ,$$
$$r_s = 2.73 \text{ fm}, \quad r_t = 1.749 \text{ fm} .$$

A proper determination of the neutron-proton diffusion coefficient D_{np} requires a solution of the transport equation because the particles have nearly equal masses. To avoid this we approximate D_{np} with the simple formula

$$D_{np} = \tfrac{1}{3} v\lambda , \tag{23}$$

where $v = (3T/M)^{1/2}$ is the speed of a thermal neutron and $\lambda = 1/n_p\sigma$ is the mean free path of a thermal neutron. This formula is exact for energy-independent s-wave scattering off fixed scattering centers. The neglect of the center-of-mass motion tends to underestimate D_{np} because it overestimates the laboratory scattering angle. The error is probably less than a factor of 2 in D_{np}, which becomes a 40% error in d/a. The diffusion coefficient is

$$D_{np} = \frac{6.53\times 10^{10}}{1-X_n} \frac{T_e^{1/2}}{\eta_8 \sigma_{np} T_\nu^3} \frac{\text{cm}^2}{\text{sec}} , \tag{24}$$

where σ_{np} is the neutron-proton cross section in fm^2, T_e and T_ν are the electron and neutrino temperatures in MeV, and $\eta_8 = 10^8\eta$, where η is the baryon-to-photon ratio at the current epoch. When the weak interactions are in equilibrium X_n is given by Eq. (8). After weak decoupling we take the constant value $X_n = \frac{1}{6}$, which is appropriate just prior to the nucleosynthesis.[19]

The most important scattering mechanism for protons is Coulomb collisions with electrons and positrons. We assume that the proton mass M_p and electron energy E_e satisfy $M_p \gg E_e$. With this, the differential cross section is

$$\frac{d\sigma}{d\Omega} = \frac{\alpha^2 m_e^2}{4k^4 \sin^4(\theta/2)} \left[1 + \frac{k^2}{m_e^2}\cos^2(\theta/2) \right] . \tag{25}$$

The transport cross section computed from Eq. (25) has the usual divergence at small scattering angles. We obtain

$$\sigma_t = 4\pi\alpha^2 \left[\frac{E_e \hbar}{k^2} \right]^2 \Lambda , \tag{26}$$

where $\Lambda = \ln(2/\theta_0)$ is the Coulomb logarithm and θ_0 is the minimum scattering angle. The diffusion coefficient D_p may be computed from Eqs. (18), (20), and (26). We find

$$D_p = \frac{3\pi}{8\alpha^2\Lambda} \left[\frac{\hbar}{m_e} \right] \frac{x e^{1/x}}{g(x)} \tag{27}$$

or, numerically,

$$D_p = \frac{2.56\times 10^4}{\Lambda} \frac{x e^{1/x}}{g(x)} \frac{\text{cm}^2}{\text{sec}} ,$$

where $x = T/m_e c^2$ and $g(x) = 1 + 2x + 2x^2$.

The scattering is cut off by Debye screening at small scattering angles. The Debye wave vector is

$$k_d^2 = \frac{4\pi e^2 n_e}{T} , \tag{28}$$

where n_e is the density of electrons plus positrons. The proton charge is screened for momentum transfer less than k_D; thus $\theta_0 = k_D/k_{\text{th}}$, where k_{th} is the mean thermal wave vector. We find that $\Lambda = 3.54$ for $T \gg m_e c^2$ and $\Lambda = 5.22$ for $T = 0.2 m_e c^2$. We adopt the constant value $\Lambda = 5$ in our calculations.

We note that the usual radiation drag formula[20] is not applicable for temperatures greater than or of order $m_e c^2$. The usual formula assumes that as protons diffuse out of a region of enhanced proton density they leave behind a net negative charge, and the resulting electric field forces the proton to drag the electrons along with them. Thus one should use the electron mobility in Eq. (18) to compute the effective proton diffusion coefficient. This argument clearly requires the ability to maintain electric fields in the plasma over distances of order the mean distance between protons, which is to say that the Debye length must exceed the mean proton separation. In the absence of thermal pairs this condition is true whenever the Debye approximation is valid. At high temperatures thermal pairs appear in sufficient numbers to short out electric fields over distances much smaller than the mean proton separation. Specifically, if r_p is the radius of a sphere containing one proton and $\lambda_D = k_D^{-1}$ is the Debye length, then for $T > m_e c^2$

$$\frac{r_p}{\lambda_D} = 74\eta_8^{-1/3} . \tag{29}$$

The protons and extra electrons that neutralize them never see one another. The thermal pairs thin out rapidly for $T < m_e c^2$. The condition $\lambda_D = r_p$ is met at $T = 40$ keV for $\eta_s = 1$ and $T = 34$ keV for $\eta_8 = \frac{1}{30}$.

Comoving diffusion lengths for neutrons and protons are shown in Fig. 1 for both the case $\eta_8 = 1$, which approximately corresponds to a closure density of baryons ($\eta_8 = 3\Omega_B h^2$), and $\eta_8 = \frac{1}{30}$, which is implied by the deuterium abundance if homogeneous nucleosynthesis is assumed. The diffusion lengths are computed from Eq. (7), with $u(t)$ defined by Eq. (4) if the weak interactions have decoupled, or by Eqs. (4) and (10) if they have not. The time dependence of the electron and neutrino temperatures are computed in the standard manner,[19] but we allow for a massless τ neutrino in our computation.

III. NEUTRON-PROTON SEGREGATION

As a matter of general principle, any fluctuation in baryon density leads to variations in the mixture of protons and neutrons at nucleosynthesis. This is simply a consequence of the fact that fluctuations in n and p relax to uniformity at different rates. Neutrons and protons above about $T_{\text{weak}} \simeq 800$ keV are continually being intertransmuted by the weak interactions, but at lower temperature the neutron component comprises a separated species which spreads out more quickly than the protons because of weaker scattering with the electron plasma. If conditions are such that this spreading takes a significant fraction of the neutrons into regions with very different mean composition, then the effects can be dramatic. Whether this segregation has any significant effect on nucleosynthesis depends on the statistical properties of the fluctuations. In practice the effects are only observable if fluctuations are nonlinear and in an appropriate range of scale. The most dramatic effects occur if the initial baryon abundance in the void (baryon-poor) region is far enough below the mean value that n can locally outnumber p at the temperature of nucleosynthesis $T_{\rm ns} \simeq 100$ keV. Let us now investigate various idealized circumstances under which neutrons might find themselves in such a region with a relatively low proton abundance.

(1) *Baryon lumps.* Suppose matter at $T_{\rm weak}$ is concentrated into lumps which occupy a small fraction of all space, with mean interlump separation $R_{\rm sep}$. The size of the lumps at $T_{\rm weak}$ is at least the baryon diffusion length at that time; $R_l \gtrsim d(T_{\rm weak})$. After $T_{\rm weak}$ the neutron component of the lumps continues to grow like d_n while the protons remain frozen at the same initial comoving size, with physical radius aR_l. Of course, the neutrons are random walking all the time and a fraction $\simeq(aR_l/d_n)$ of them happen to walk back into the proton lump once in a Hubble time (we have used the fact that Brownian walks are two-dimensional fractals). For $aR_l < R_{\rm sep} < d_n$, the neutron clouds from different lumps overlap and the fraction of neutrons hitting a lump per Hubble time is $(d_n/R_{\rm sep})^3(aR_l/d_n)$. A large fraction of neutrons undergo nucleosynthesis in neutron-dominated regions if

$$aR_l \ll d_n(T_{\rm ns})$$

and (30)

$$aR_l d_n(T_{\rm ns})^2 \ll R_{\rm sep}{}^3 \; .$$

This is valid for a wide range of plausible R_l and $R_{\rm sep}$, which includes the range of $R_{\rm sep}$ expected on the basis of naive nucleation theory for the QCD phase transition[11] (see Fig. 1).

(2) Plane geometry. Next, consider a "baryon slab" separated from a region devoid of baryons by a plane. A "fog" of neutrons gathers above the slab as they diffuse away from the protons. As nucleosynthesis within the slab becomes more frequent at about $T_{\rm ns}$, neutrons which cross the boundary back into the slab are likely to get "stuck" in nuclei which no longer diffuse. Let us assume perfect sticking and ask what fraction would be left in the neutron-rich zone. Standard results on changes of sign of a one-dimensional random walk[21] can be used to estimate the fraction remaining after a time H^{-1} has elapsed, corresponding to those which never go back across the boundary. The expected number of zero crossings only increases as $\sqrt{t}$ and the chance of no crossings is surprisingly large, of order

$$\langle N \rangle \simeq (MbH)^{1/4} \tag{31}$$

which after nucleosynthesis begins might be a few percent. As we shall see, this is large enough to be interesting, since the net deuterium abundance is not sensitive to the fraction of neutrons participating in neutron-rich zones unless this fraction becomes very small.

(3) *Baryon voids.* Finally, consider a spherical baryon void. Suppose regions of radius R_V have been evacuated of the bulk of their baryons (this means enough of them in order for diffusing neutrons to dominate over residual void protons at $T_{\rm ns}$; this implies that voids must be less than about 0.08 of the mean density since 0.16 of baryons are neutrons after $T_{\rm weak}$ and these must be about twice as abundant as void protons for the effect described below to occur). If $R_V > d_n$, this reduces to the slab case. But if $R_V < d_n$, and we again assume that neutrons are eaten as they cross the boundary, then they are rapidly (exponentially) depleted. Thus voids must be above the minimum comoving size $d_n(T_{\rm ns})$ to produce interesting effects from free neutrons; this is much more stringent than the scale restriction for lumps. Of course, if structures are very much larger than d_n, only a small fraction of the matter is within d_n of a boundary, so the effects again become unimportant.

Thus highly concentrated "lumplike" structures would typically lead to neutron-rich zones for $R_{\rm sep} \gtrsim 10^{3.5}$ cm $[T\,({\rm MeV})]^{-1}$; to have the same effect, voidlike structures must exceed $d_n(T_{\rm ns}) \simeq 10^5$ cm $[T\,({\rm MeV})]^{-1}$ in size, but not by many orders of magnitude. Either case is plausible for fluctuations produced in the QCD phase transition, for which the horizon scale is $3\times10^8\,[T\,({\rm MeV})]^{-1}$ cm and the plausible nucleation scale is perhaps 1% of this, $R_{\rm sep} \lesssim 3\times10^6[T\,({\rm MeV})]^{-1}$ cm. The electroweak phase transition, for which the horizon scale H^{-1} is $3\times10^5[T\,({\rm MeV})]^{-1}$ cm could also conceivably generate perturbations of appropriate scale and geometry to cause the same effects.

It is more difficult at present to know what fraction of baryons would be expected to be in nonlinear structures. The simple transport theory of Ref. 9 predicts that nonlinear entropy fluctuations are generated when the temperature gradient between the phases $(\delta T/T)$ is of order unity. This in turn is expected to occur in quasistatic equilibrium when the total surface area available for transport within a volume $(c/H)^3$ is of order $(c/H)^2$ or less. Since the largest bubbles of size $\simeq R_{\rm sep}$ are the last to evaporate, the total surface area of such bubbles is $(c/H)^2$ when a fraction $\simeq(R_{\rm sep}H/c)$ of the matter has yet to change phase. But these evaporate in a fraction $(R_{\rm sep}H/c)^{1/2}$ of a Hubble time so the quark matter is all gone before the Universe expands to $\delta T/T=1$; there may be no nonlinear fluctuations in entropy. On the other hand, a strongly supercooled detonation[22] or Higgs vacuum transition would naturally produce strong nonlinearities. Therefore, one must bear in mind that while the scale of fluctuations (which is easy to predict on general grounds) is correct, the amplitude (which is dependent on many unknown properties of the transition) is not known definitely to be either interestingly large or negligibly small.

IV. NUCLEOSYNTHESIS IN NEUTRON-RICH REGIONS

We now investigate in some detail the nuclear reactions which occur with segregated neutrons in the big bang. The previous discussions have demonstrated a number of situations where neutrons can outnumber protons in some regions of space. Here we work with the simplest possible model of such a region: assume that it is homogeneous, and that it is composed either entirely of neutrons to begin with or of a fraction F_n of neutrons with a small admixture of residual protons. These neutrons are allowed to decay into protons, and all of the other standard nucleosynthesis reactions occur as usual. We calculate quantitatively the nuclear abundance ratios produced under these conditions, and the dependence of abundances on entropy and on any small proton contamination, by running a modified version of Wagoner's[23] nucleosynthesis code, with updated reaction rates.[24,25] We begin initially with pure neutrons, and we "turn off" the weak interactions which interconvert neutrons and protons (with the exception of neutron decay) to simulate the fact that neutrons diffuse into the underdense regions after these weak-interaction rates have dropped below the expansion rate and are no longer important. We assume that the baryon-photon ratio in the neutron-rich regions is constant during nucleosynthesis, and that the baryon density in these regions red-shifts as R^{-3}. These assumptions will be valid as long as the decrease in neutron density due to diffusion does not dominate the decrease due to Hubble expansion. This requires, in effect, that the neutron clouds from adjacent lumps have overlapped, so that the void regions are filled uniformly with neutrons. When diffusion dominates the Hubble expansion, the baryon density in the neutron-rich regions will decrease more rapidly than a^{-3}, and the baryon-photon ratio will decrease with time, but we expect many of our results would not be very much changed by this.

We characterize the initial baryon density perturbations and the diffusion using a simple model which collapses many of the complicating effects described in the previous two sections and enables us to obtain simple expressions for final net element abundances in terms of two parameters: f_n and f_V. Let $n/(n+p)$ be the ratio of neutrons to baryons when the neutrons first start behaving like a separate component, so that in principle this is the maximum fraction of baryons available for neutron-rich nucleosynthesis. (Some ambiguity in what precise epoch to adopt leads to a numerical ambiguity of order unity, which is unavoidable since we have not self-consistently solved for the statistical properties of simultaneously intertransmuting and diffusing baryons in a particular geometry.) We adopt a value of $\frac{1}{6}$ for this quantity which is the freeze-out neutron abundance in the standard model with neutron decay turned off completely. Now divide space into "void" regions with no baryons initially, and "lump" regions where the protons (comprising $\frac{5}{6}$ of the net baryon abundance) remain throughout nucleosynthesis. Assume that a fraction $f_n \lesssim 1$ of the neutrons actually diffuses into the void regions before nucleosynthesis and undergoes homogeneous nucleosynthesis as in our calculations. Let f_V be the fraction of the total volume of space occupied by the diffusing neutrons during nucleosynthesis. Then $f_V \lesssim 1$, with $f_V = 1$ when the neutron clouds from adjacent lumps have overlapped and the volume of space occupied by the lumps is negligible. The element abundances in the calculations are expressed as a function of $\eta_{\rm ns}$, the baryon-photon ratio in the neutron-rich regions during nucleosynthesis. This will differ from the mean baryon-photon ratio η_0 because only a fraction of the baryons diffuse into the void regions in the form of neutrons:

$$\eta_0 = \eta_{\rm ns} f_V \left[\frac{n}{n+p} \right]^{-1} f_n^{-1} \; . \tag{32}$$

This simple model is a fairly accurate representation of what occurs in the case of widely separated, highly concentrated baryon lumps with $R_{\rm sep} \lesssim d_n(T_{\rm ns})$.

The various element abundances produced in the neutron-rich regions are calculated as a mass fraction $X_{\rm ns}$ relative to the mass of baryons in these regions during nucleosynthesis. This will contribute to the observed mean mass fraction today X_0 an amount

$$X_0 = X_{\rm ns} \left[\frac{n}{n+p} \right] f_n \; . \tag{33}$$

Table I gives the mass fractions $X_{\rm ns}$ for a variety of light elements as a function of $\eta_{\rm ns}$. The time evolution of the element abundances for two values of the baryon-photon ratio is shown in Figs. 2(a) and 2(b). It is clear that for most values of $\eta_{\rm ns}$, almost all of the baryons in the neutron-rich regions end up in ^{4}He. Then from Eq. (33), the helium-4 abundances today will simply be

$$X_0(^4{\rm He}) = \frac{n}{n+p} f_n \; , \tag{34}$$

plus a contribution from the "normal" regions with protons. This implies that the neutron-rich contribution is $X_0(^4{\rm He}) \sim 16\%$ when $f_n \sim 1$. Although nearly all of the

TABLE I. Products of neutron-rich cosmological nucleosynthesis ($F_n = 1$).

$\eta_{\rm ns}$	$X_{\rm ns}(^4{\rm He})$	$\log_{10} X_{\rm ns}(^2{\rm H})$	$\log_{10} X_{\rm ns}(^3{\rm He})$	$\log_{10} X_{\rm ns}(^7{\rm Li})$	$\log_{10} X_{\rm ns}(A \geq 12)$	$\log_{10}(\eta X_D)$
10^{-11}	28.5%	−1.76	−3.14	−7.47	−13.42	−12.8
10^{-10}	81%	−2.5	−3.7	−6.7	−10.3	−12.5
10^{-9}	96%	−3.3	−4.5	−6.6	−7.7	−12.3
10^{-8}	99%	−4.1	−5.3	−6.7	−5.5	−12.1
10^{-7}	100%	−5.0	−6.1	−6.7	−4.0	−12.0
10^{-6}	100%	−5.9	−7.0	−6.8	−2.8	−11.9
10^{-5}	98%	−6.7	−7.9	−6.9	−1.7=2%	−11.7
10^{-4}	82%	−7.2	−8.5	−7.3	(18%)	−11.2

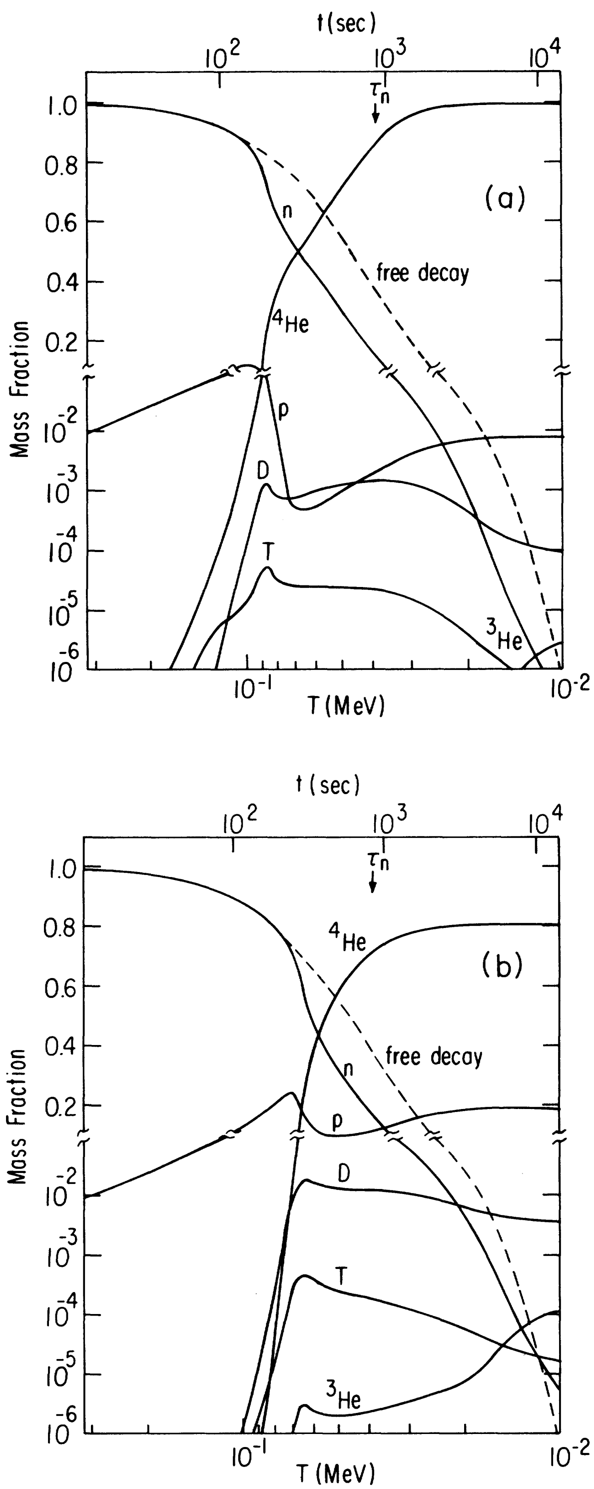

FIG. 2. (a) Evolution of cosmic abundances in a medium initially dominated by neutrons with $\eta_{\rm ns}=10^{-8}$. Mass fraction is shown as a function of temperature/time for various species. The top portion is a linear plot, the bottom portion logarithmic. The dashed line gives the neutron abundance in the absence of all reactions other than neutron decay. Note the secondary peak in D production at about τ_n, the neutron half-life. (b) Same as (a), but with $\eta=10^{-10}$.

neutrons are converted into helium, the net effect is a *reduction* in total helium from the standard model of the same mean η. This is because the same initial number of neutrons in the standard model can produce twice the final helium mass by reacting with the primordial protons, rather than protons which have been produced by decaying neutrons. Since half of the void neutrons are thereby "wasted" we find that, in the limit $f_n \ll 1$,

$$\frac{\delta Y}{Y} \simeq \left[\frac{X_{\rm ns}(^4{\rm He})-2}{2}\right] f_n \simeq -f_n/2 \qquad (35)$$

is the fractional reduction in net remixed ^{4}He mass fraction from the standard model, where $X_{\rm ns}(^4{\rm He})$ is taken from Table I. If $f_n \approx 0.2$, this would provide a natural explanation of a number of measurements (cited in Ref. 2) of $X_0(^4{\rm He})$ which appear too low ($\lesssim 23\%$) to be consistent with any plausible value of Ω_b in the homogeneous picture.

The deuterium abundance produced in this model for large values of $\eta_{\rm ns}$ is significantly greater than in the standard model. This is because of the larger abundance of neutrons at late times in this model which enables deuterium manufacturing reactions to compete better with deuterium burning reactions. Figure 2(a) actually shows a second maximum in D abundance, presumably as a result of protons becoming available from neutron decay. The deuterium abundance varies inversely with the baryon-photon ratio at nucleosynthesis: $X_{\rm ns}(^2{\rm H})\eta_{\rm ns} \sim 10^{-12}$ (see the last column of Table I). The consequence is that the relation between the deuterium abundance today and the baryon-photon ratio today is independent of many details of the neutron diffusion. From Eqs. (32) and (33)

$$X_0(^2{\rm H})\eta_0 = X_{\rm ns}(^2{\rm H})\eta_{\rm ns} f_V \sim 10^{-12} f_V \ . \qquad (36)$$

Thus the present deuterium abundance depends only on the current baryon-photon ratio and the fraction of space occupied by the diffusing neutrons during nucleosynthesis; it is almost independent of the fraction of baryons which diffuse as neutrons into the void regions. The requirement that $X_0(^2{\rm H}) \sim 3\times10^{-5}$ yields $\eta_0 \sim 3\times10^{-8} f_V$. Thus $\Omega_b \sim 1$ can be consistent with the observed deuterium abundance for $f_V \sim 0.25-1$ depending on h ($\eta_0 = 3\times10^{-8}\Omega h^2$):

$$X_0(^2{\rm H}) \simeq 3\times10^{-5} f_v/\Omega_b h^2 \ .$$

In this model the observed deuterium abundance provides a constraint on the present baryon-photon ratio and on f_V but gives no information on the details of neutron diffusion (f_n), while the ^{4}He abundance is quite insensitive to the present baryon-photon ratio and depends primarily on the fraction of baryons $f_n[n/(n+p)]$ which diffuse into the void regions.

This model can yield ^{4}He and deuterium abundances in good agreement with the observations over a wide range of Ω_b. Interpretation of observed ^{3}He and ^{7}Li abundances is not as straightforward, however. The ratio of ^{3}He to ^{2}H produced in the neutron-rich regions is a constant independent of the baryon-photon ratio and all of the diffusion parameters:

$$X_{\rm ns}(^3{\rm He})/X_{\rm ns}(^2{\rm H}) \approx 6\times10^{-2} \ . \qquad (37)$$

The observations suggest $X_0(^2\mathrm{H}) \approx X_0(^3\mathrm{He})$, so our model underproduces ^{3}He. However, ^{3}He is easily produced in a number of astrophysical sources, so underproduction is not a problem; modest astrophysical reprocessing could explain the observations.

A potentially more serious ambiguity arises with the ^{7}Li abundance. The ^{7}Li produced in neutron-rich regions contributes $X_0(^7\mathrm{Li})$ about 2×10^{-7} times the ^{4}He contribution from these regions. This is generally (except for $f_n \ll 1$) a significant increase over the standard model of the same entropy. The observations of Spite *et al.*[26,27] indicate a ^{7}Li mass fraction of $\simeq 10^{-9}$ in a sample of metal-deficient population II subdwarfs. On the one hand, these observations indicate a surprising uniformity in stars with different properties, which might be taken as evidence of a pristine primordial abundance, but on the other hand, it has long been thought that dwarfs in general might destroy Li very efficiently, which would tend to make them deficient in Li relative to the primordial value. Other places, such as meteorites, population I stars, and the interstellar medium, have considerably higher values.[1] Boesgaard and Steigman[1] argue that the population I value is possibly the primordial one, especially since it is so constant in a great variety of objects. Confirmation of high primordial levels of Li might come from better knowledge of the ^{6}Li/^{7}Li isotopic ratio. Our model yields ^{7}Li abundances a factor of about $200 f_n[n/(n+p)]$ times the population II observations and a factor $\sim 30 f_n[n/(n+p)] \simeq 5 f_n$ times greater than the larger population I value of 7×10^{-9} by mass. Either the primordial ^{7}Li abundance is considerably higher than the population II observations, or else inhomogeneous models of this sort with neutron-rich regions having $f_n \gtrsim 0.03$ can be ruled out. On the other hand, it is worth noting that a model with $\Omega_b = 1$, $h^2 = 0.25$, and $f_n \sim f_V \sim 0.2$ would be able to accommodate population I Li, D, and ^{4}He simultaneously.

Another interesting and unexpected result of these calculations is a very large increase in heavy elements relative to the standard model. Table I, for example, shows that $X_{\mathrm{ns}}(A \geq 12)$—the total mass fraction in carbon and all heavier elements— is $10^{-5.5}$ for $\eta_{\mathrm{ns}} = 10^{-8}$, whereas standard nucleosynthesis at the same baryon number predicts $X(A \geq 12) < 10^{-12}$. Most of this mass was in ^{14}C, which decays to ^{14}N. The net mixed abundance of heavier elements is obtained by multiplying $X_{\mathrm{ns}}(A \geq 12)$ in the table by $[n/(n+p)] f_n$, which leads to a net heavy-element abundance of $\approx 10^{-6} f_n$ for $\Omega_b h^2 = 1$. At this level of enrichment, one may start to consider these elements as useful cosmological probes; for $f_n \simeq 0.3$, this abundance is comparable to the observed enrichment in the record-holding ultrametal-deficient red giant CD-38°245 (Ref. 28). It does not appear to us that such a primordial enrichment of heavy elements could solve the well-known "G-dwarf problem," or paucity of metal-poor stars, since what we actually predict is a universal cosmic "floor" abundance of heavy elements and this has not been observed. Rather, what has been found is that very metal-poor stars are also very rare, and the extreme example just cited is much less enriched than the next-poorest star.[29] Of course, more such ultradeficient stars might be found in the future and such a "floor" abundance might be found. Therefore, we are proceeding to calculate the element and isotope abundance ratios of these heavier elements so that a quantitative comparison can be made with abundances in population II stars. Currently, stellar spectra provide separate abundance estimates for about a dozen elements and show a marked deviation from solar relative abundances. At the moment our numerical calculations stop at O^{16} and we cannot reliably estimate even the carbon-to-oxygen ratio.

What is the effect of neutrons diffusing back into the lumps? The effect in the void regions will simply be a smaller value for f_n, giving a smaller value for η_{ns}. Since we take f_n and η_{ns} to be free parameters, we have effectively already included this in our calculations. However, the diffusion of neutrons back into the lumps, as well as the presence of neutrons which never diffuse out of the lumps, raises the possibility of nucleosynthesis in the proton-enriched lump regions. The production of the other light elements in neutron-poor, low-entropy lump regions should be similar to nucleosynthesis in low-energy models of the Universe with large positive neutrino degeneracy[30,31] where the neutron fraction is below normal. These results indicate a negligible production of the light elements of interest, but they also suggest that the production of heavy ($A \geq 12$) elements could be significant in the lumps.

If the void regions are not completely empty to begin with, the neutrons diffusing into the voids will encounter a nonzero initial abundance of protons. To determine the sensitivity of nucleosynthesis to such an effect, we have calculated the final element abundances using initial neutron mass fractions <1. The results for $\eta_{\mathrm{ns}} = 10^{-8}$ are

TABLE II. Sensitivity of element abundances to initial neutron fraction F_n for $\eta_{\mathrm{ns}} = 10^{-8}$.

F_n	$X_{\mathrm{ns}}(^4\mathrm{He})$	$\log_{10} X_{\mathrm{ns}}(^2\mathrm{H})$	$\log_{10} X_{\mathrm{ns}}(^3\mathrm{He})$	$\log_{10} X_{\mathrm{ns}}(^7\mathrm{Li})$	$\log_{10} X_{\mathrm{ns}}(A \geq 12)$
1	99%	−4.1	−5.3	−6.7	−5.5
0.9	99%	−4.1	−5.4	−6.6	−5.5
0.8	99%	−4.2	−5.3	−6.6	−5.6
0.7	99%	−4.2	−5.4	−6.6	−5.8
0.6	99%	−5.2	−6.0	−8.4	−9.1
0.5	83%	−6.4	−5.5	−7.2	−10.4
0.4	67%	−7.6	−5.3	−7.1	−10.8
0.3	50%	−8.9	−5.2	−7.1	−11.1

TABLE III. Primordial element mass fractions.

Element	Standard model $\Omega_b h_{50}^2=1$	Standard model $\Omega_b h_{50}^2=0.1$	Segregated model $\Omega_b h_{50}^2=1$	"Observed (?)"
^{4}He	0.26	0.24	$0.26(1-f_n/2)$	0.24 ± 0.01
^{2}He	10^{-8}	4×10^{-5}	$1.2\times10^{-4}f_V$	$\gtrsim3\times10^{-5}$
^{3}He	4×10^{-6}	2×10^{-5}	$7.2\times10^{-6}f_V$	$\lesssim6\times10^{-5}$
^{7}Li	1.7×10^{-8}	1.2×10^{-9}	$3.5\times10^{-8}f_n$	7×10^{-9} Pop I
				8×10^{-10} Pop II
$A\geq12$	$<10^{-12}$	$<10^{-12}$	$10^{-6}f_n$	$\lesssim10^{-6.5}$

given in Table II. The final element abundances are insensitive to an initial proton mass fraction as large as 30%, but larger initial proton mass fractions begin to alter the element abundances significantly. At this point the idealized model we have used to describe nucleosynthesis begins to break down.

In Table III we compare the net abundances derived from our calculations and the simple model of this section to standard-model predictions[23] and to a crude distillation of observations.[1,2,28] Whereas in the standard model one finds a low value of $\Omega_b h^2$ determined securely by observations, in our segregated model it appears that present observations can accommodate any value of $\Omega_b h^2$ up to ≈ 1 with suitable choices for f_v and f_n. However, this model with $\Omega_b h_{50}^2 \simeq 1$ predicts a much higher value for primordial ^{7}Li and for primordial heavy elements than the standard model with $\Omega_b h^2 \ll 1$.

V. EPILOGUE

We have established that, in principle, a plausible mechanism exists which would enable high-baryon-density universes to mimic low-baryon-density abundances of deuterium and helium. Is it possible to go beyond our highly idealized model and make a really precise calculation of abundance perturbations? To do so would require accurate knowledge of several complex processes. First, the physics of the QCD and electroweak phase transitions would have to be thoroughly understood; this means not just a knowledge of the order of the transitions, but of the surface tension between phases and the shape of the effective potential governing nucleation. The nonlinear baryon perturbations could then be calculated in principle, although this would involve two-phase nonspherical, nonlinear radiative hydrodynamics. Neutron transport would be calculated in similar circumstances, and finally nucleosynthesis reactions would need to be integrated in this inhomogeneous medium simultaneously with the transport effects. Clearly idealized models of some sort are necessary for the foreseeable computational future.

Considerable progress might be made in calculating the general features of nonlinearities from the QCD transition. The gross features of its nucleation are already understood; establishing that it is first order and calculating the surface tension would fix the supercooling at nucleation and many features of the radiative transport. Lattice QCD shows excellent promise of providing this foundation. Knowledge of the electroweak transition may be considerably longer in coming. A naive estimate of the nucleation scale—1% of the Hubble length at 100 GeV—falls just short of the proton diffusion length, so electroweak bubbles might only be on the edge of producing any segregation effects of all. On the other hand, such a naive estimate might be wildly wrong—for example, in the Coleman-Weinberg–based scenario of Witten,[32] electroweak bubbles would coincide with QCD bubbles and be of comparable size. Any number of unrelated mechanisms[33,34] may also generate nonlinear baryon inhomogeneity at $\lesssim 100$ GeV, which are likely to lie in the right range of scales for these segregation effects to be important. The fact that this scale is now considered to be the threshold for supersymmetric effects leaves open the possibility of other radically new schemes.

Reliable modeling is also difficult because in some sense the effects may be intrinsically small—even though the perturbations to D abundances are large, the total nucleosynthetic yield (primarily in helium) need not be changed appreciably, and only a small fraction of the matter need participate if f_n is small. One of the most attractive features of this scheme is that it preserves the essentially good agreement[1] between big-bang nucleosynthesis and observation which is the cornerstone of the standard model. Conversely, observational deviations from the $\Omega_b = 1$ standard model are likely to remain difficult to interpret unambiguously. The conventional interpretation that $\Omega_b < 1$ based on exact homogeneity is still the simplest one but our conclusions suggest that this interpretation should not be given undue weight. It could simply be that the standard homogeneous nucleosynthesis model is a good first approximation to a description of the actual early Universe, but slight discrepancies arise from effects such as those we have discussed here. There is certainly precedent for this type of situation in other astrophysical systems.

ACKNOWLEDGMENTS

We thank R. V. Wagoner for the use of his computer code, and we are grateful to E. W. Kolb, J. Liebert, and R. Peterson for helpful discussions. This work was supported by NASA Theoretical Astrophysics Grant No. NAGW-763 at the University of Arizona, DOE Contract No. ACO2-80ER-10773, and a McCormick Foundation (R.J.S.) at the University of Chicago. One of us (C.J.H.) wishes to thank the Alfred P. Sloan Foundation for support.

[1]J. Yang, M. S. Turner, G. Steigman, D. N. Schramm, and K. Olive, Atrophys. J. **281**, 493 (1984); A. Boesgaard and G. Steigman, Annu. Rev. Astron. Astrophys. **23**, 319 (1985).

[2]B. Pagel, in *Inner Space/Outer Space,* edited by E. W. Kolb *et al.* (University of Chicago, Chicago, 1986), p. 72; B. J. Pagel, Philos. Trans. R. Soc. London **A307**, 19 (1982).

[3]Yu. K. Melik-Alaverdian, Astrofizika **10**, 123 (1974) [Astrophysics **10**, 77 (1974)].

[4]L. M. Ozernoy and V. V. Chernomordnik, Astron. Zh. **52**, 1156 (1975) [Sov. Astron. **19**, 693 (1975)].

[5]R. J. Scherrer, Mon. Not. R. Astron. Soc. **210**, 359 (1984).

[6]J. Audouze, D. Lindley, and J. Silk, Astrophys. J. **293**, L53 (1985).

[7]S. Ramadurai and M. J. Rees, Mon. Not. R. Astron. Soc. **214**, 53P (1984).

[8]R. Epstein and V. Petrosian, Astrophys. J. **197**, 281 (1975).

[9]J. H. Applegate and C. J. Hogan, Phys. Rev. D **31**, 3037 (1985); **34**, 1938(E) (1986).

[10]E. Suhonen, Phys. Lett. **119B**, 81 (1982).

[11]C. Hogan, Phys. Lett. **133B**, 172 (1983).

[12]E. Witten, Phys. Rev. D **30**, 272 (1984).

[13]Some of the early work of Gamow and collaborators in the 1940s also considered neutron-rich universes. For a history of this work, see R. A. Alpher and R. Herman, in *Cosmology, Fusion and Other Matters,* edited by F. Reines (Colorado Associated Press, Boulder, 1972), p. 1.

[14]L. D. Landau and E. M. Lifschitz, *Fluid Mechanics* (Pergamon, New York, 1959).

[15]P. J. E. Peebles, Astrophys. J. **146**, 542 (1966).

[16]I. J. R. Aitchison and A. J. G. Hey, *Gauge Theories in Particle Physics: A Practical Introduction* (Adam Hilger, Bristol, U.K., 1982).

[17]L. D. Landau and E. M. Lifschitz, *Physical Kinetics* (Peragamon, New York, 1981).

[18]M. A. Preston and R. K. Bhaduri, *Structure of the Nucleus* (Addison-Wesley, Reading, MA, 1975).

[19]S. Weinberg, *Gravitation and Cosmology* (Wiley, New York, 1972).

[20]P. J. E. Peebles, *Physical Cosmology* (Princeton University, Princeton, NJ, 1971).

[21]W. Feller, *An Introduction to Probability Theory and its Applications,* 2nd ed. (Wiley, New York, 1968), Vol. 1, pp. 84ff.

[22]T. Degrand and K. Kajantie, Phys. Lett. **147B**, 273 (1984).

[23]R. V. Wagoner, Astrophys. J. **179**, 343 (1973).

[24]W. A. Fowler, G. R. Caughlan, and B. A. Zimmerman, Annu. Rev. Astron. Astrophys. **13**, 69 (1975).

[25]M. J. Harris, W. A. Fowler, G. R. Caughlan, and B. A. Zimmerman, Annu. Rev. Astron. Astrophys. **21**, 165 (1983).

[26]F. Spite and M. Spite, Astron. Astrophys. **115**, 357 (1982).

[27]M. Spite, J. P. Maillard, and F. Spite, Astron. Astrophys. **141**, 56 (1984).

[28]M. S. Bessel and J. Norris, Astrophys. J. **285**, 622 (1984).

[29]T. C. Beers, G. W. Preston, and S. A. Shectman, report, 1986 (unpublished).

[30]R. J. Scherrer, Mon. Not. R. Astron. Soc. **205**, 683 (1983).

[31]N. Terasawa and K. Sato, Astrophys. J. **294**, 9 (1985).

[32]E. Witten, Nucl. Phys. **B177**, 477 (1981).

[33]M. Fukugita and V. A. Rubakov, Phys. Rev. Lett. **56**, 988 (1986).

[34]I. Affleck and M. Dine, Nucl. Phys. **B249**, 361 (1985).